Caspase-2 functions upstream of mitochondria in endoplasmic reticulum stress-induced apoptosis by bortezomib in human myeloma cells

Hongtao Gu, Xiequn Chen, Guangxun Gao, and Hongjuan Dong

Department of Hematology, Xijing Hospital, Fourth Military Medical University, Xi'an, People's Republic of China

Abstract

Multiple myeloma is an incurable plasma cell malignancy. The 26S proteasome inhibitor, bortezomib, selectively induces apoptosis in multiple myeloma cells; however, the mechanism by which this compound acts remains unknown. Here, we, using immunoblotting analysis, observed that the expression of BiP, CHOP, and XBP-1 is up-regulated in bortezomib-induced apoptosis in human multiple myeloma cell lines NCI-H929 and RPMI-8226/S, strongly suggesting that endoplasmic reticulum (ER) stress response or the unfolded protein response (UPR), a signaling pathway activated by the accumulation of unfolded proteins within ER, is initiated. In the meantime, we also showed that bortezomib inhibited classic ER stressor brefeldin A–induced up-regulation of prosurvival UPR components BiP and XBP-1, resulting in increased induction of apoptosis in multiple myeloma cell lines, raising the possibility that bortezomib induces apoptosis of multiple myeloma cells by means of evoking the severe ER stress but disrupting the prosurvival UPR required. Using caspase inhibitors and a RNA interference approach, we finally confirmed that bortezomib-triggered apoptosis in multiple myeloma cells is dependent on caspase-2 activation, which is associated with ER stress and required for release of cytochrome *c*, breakdown of mitochondrial transmembrane potential, and its downstream caspase-9 activation. Taken together, these data strongly suggest that caspase-2 can serve as a proximal caspase that functions upstream of mitochondrial signaling during ER stress-induced apoptosis by bortezomib in multiple myeloma cells. [Mol Cancer Ther 2008;7(8):2298–307]

Received 2/27/08; revised 5/19/08; accepted 5/28/08.

Grant support: Sci-tech Research Project of Shannxi Province, China, grant 2007K09-09.

The costs of publication of this article were defrayed in part by the payment of page charges. This article must therefore be hereby marked *advertisement* in accordance with 18 U.S.C. Section 1734 solely to indicate this fact.

Requests for reprints: Xiequn Chen, Department of Hematology, Xijing Hospital, Fourth Military Medical University, 17 Changle West Road, Xi'an 710032, People's Republic of China. Phone: 86-29-84775199; Fax: 86-29-82558905. E-mail: xiequnchen@fmmu.edu.cn

doi:10.1158/1535-7163.MCT-08-0186

Introduction

Bortezomib (Velcade, formerly PS-341), a specific and selective inhibitor of 26S proteasome (1), has shown remarkable therapeutic efficacy in multiple myeloma, a plasma cell malignancy (2–6). However, the mechanism by which this drug acts remains unknown. Previous reports have showed that proteasome inhibition by bortezomib abrogates degradation of IκB, leading to the cytoplasmic sequestration and inhibition of the transcription factor nuclear factor-κB (3, 7–9). Although constitutive nuclear factor-κB activity in multiple myeloma cells has been shown to increase multiple myeloma cell survival and resistance to cytotoxic agents (10), bortezomib was shown to have more profound effects on multiple myeloma cell proliferation than a specific IκB kinase inhibitor, PS-1145 (7), suggesting that nuclear factor-κB inhibition cannot completely explain the nature of the selectivity of bortezomib for multiple myeloma cells.

Multiple myeloma cells produce and secrete abundant immunoglobulin. This requires a highly developed endoplasmic reticulum (ER) and production of chaperone proteins that effect proper translation and folding (11). A signaling pathway called the unfolded protein response (UPR), or ER stress response, ensures that the plasma cells can handle the proper folding of proteins and prevent the aggregation of the accumulating misfolded proteins (12). These misfolded proteins are recognized by ER quality-control systems and targeted for ER-associated protein degradation, which involves the retrograde translocation of the misfolded proteins out of the ER and subsequent degradation by cytosolic 26S proteasomes (13–15). Treatment of multiple myeloma cells with proteasome inhibitors results in the accumulation of misfolded proteins within ER, thereby inducing severe ER stress response and proapoptotic UPR signaling, which eventually lead to the induction of apoptosis (12, 16, 17). It thus has been shown that multiple myeloma cells are more sensitive than other cell types to proteasome inhibition because of their large volume of immunoglobulin production (18), which appears to lower their threshold for induction of proapoptotic UPR following any additional stress to the ER.

The role and placement of caspase-2 in stress-induced apoptotic signaling have been the focus of many studies, but a detailed molecular description of this cell death pathway has yet to emerge. Recent reports have observed activation of caspase-2 in several settings where it has been implicated, including genotoxic stress (19–21), ER stress (22–26), and heat stress (27, 28). Moreover, it was suggested that caspase-2 activation is required for mitochondrial outer membrane permeabilization and loss of mitochondrial transmembrane potential ($\Delta\Psi_m$) in response

to DNA-damaging agents and heat shock (19–21). Other reports suggested that caspase-2 can also been activated by caspase-9 in genotoxic stress-induced apoptosis (29), indicating that it can function downstream of mitochondria and cannot bypass the apoptosome during apoptotic signaling. Thus, there is conflicting evidence of whether caspase-2 activation occurs upstream or downstream of mitochondria during stress-induced apoptosis. As for the relevance of caspase-2 to ER stress-induced apoptosis of multiple myeloma cells by bortezomib, it is as of yet unknown, although several groups have implicated caspase-2 in ER stress-induced apoptosis in nonhematologic malignancies (22–26).

Here, we determined the relationship of ER stress and caspase-2 activation to mitochondrial apoptotic signaling induced by bortezomib in human multiple myeloma cell lines. Our results indicated that bortezomib, like classic ER stressor brefeldin A, triggered UPR signaling and induced ER stress-initiated apoptosis. Using caspase inhibitors and via RNA interference, we furthermore confirmed that bortezomib-triggered apoptosis was dependent on ER stress-induced caspase-2 activation. Finally, analysis of mitochondrial events showed that caspase-2 was not only required for $\Delta\Psi_m$ loss but also required for cytochrome *c* release and its downstream caspase-9 activation. Taken together, these data strongly suggest that caspase-2 functions upstream of mitochondria in ER stress-induced apoptosis by bortezomib in multiple myeloma cells.

Materials and Methods

Cell Culture

Human multiple myeloma cell lines NCI-H929 (H929) and RPMI-8226/S (8226/S) were obtained from the American Type Culture Collection. H929 and 8226/S cells were maintained in RPMI 1640 supplemented with 10% FCS, 100 units/mL penicillin, and 100μg/mL streptomycin. Packaging cell line 293FT, which were purchased from Invitrogen, grown in (high-glucose) DMEM supplemented with 10% FCS and 500 μg/mL G418 (Sigma-Aldrich).

Reagents

Bortezomib was kindly provided as a pure substance by Millennium Pharmaceuticals and dissolved in DMSO. Mouse monoclonal primary antibodies used were anti-caspase-2, anti-immunoglobulin binding protein (BiP; BD PharMingen), anti-caspase-9 (Cell Signaling Technology), and anti-β-actin (Sigma-Aldrich). Rabbit polyclonal primary antibodies used were anti-poly(ADP-ribose) polymerase, anti-cytochrome *c* (Cell Signaling Technology), and anti-CCAAT/enhancer-binding protein-homologous protein (CHOP) and anti-X-box-binding protein 1 (XBP-1; Santa Cruz Biotechnology). As secondary reagents, horseradish peroxidase–conjugated goat anti-mouse or mouse anti-rabbit antibodies (Sigma-Aldrich) were used. The broad-spectrum caspase inhibitor benzyloxycarbonyl-Val-Ala-Asp(-OMe)-fluoromethylketone (zVAD.fmk) and caspase-2 and caspase-9 inhibitors benzyloxycarbonyl-Val-Asp(-OMe)-Val-Ala-Asp(-OMe)-fluoromethylketone (zVDVAD.fmk) and benzyloxycarbonyl-Leu-Glu(-OMe)-His-Asp(-OMe)-fluoromethylketone (zLEHD.fmk), respectively, were purchased from R&D Systems. ER stress inducer brefeldin A and tunicamycin were obtained from Sigma-Aldrich.

Growth Inhibition Assay

A 100 μL suspension of 5×10^3 cells was added to each well of 96-well, flat-bottomed plates (Costar). After 24 h, various concentrations of bortezomib were added to the cells. After 24 h of incubation, growth inhibition was assessed by 3-(4,5-dimethylthiazol-2-yl)-2,5-diphenyltetrazolium bromide (Sigma-Aldrich) assay as described previously (30). Absorbance values, measured at 540 nm, were expressed as a percentage of untreated controls. The concentrations resulting in cell growth inhibition of 50% (IC_{50}) were calculated.

Subcellular Fractionation

Cytosolic and mitochondrial fractions were generated using a previously described digitonin-based subcellular fractionation technique (31). In brief, cells were harvested, washed in ice-cold PBS (pH 7.2), and lysed at a density of 3×10^7/mL in a permeabilization buffer [210 mmol/L D-mannitol, 70 mmol/L sucrose, 10 mmol/L HEPES, 5 mmol/L sodium succinate, 200 μmol/L EGTA, 0.15% FCS, 1× protease inhibitor cocktail (Roche Diagnostics), 250 μmol/L phenylmethylsulfonyl fluoride, and 80 μg/mL digitonin] on ice for 5 min. The lysate was centrifuged at 750 rpm for 5 min at 4°C to remove nuclear material and unlysed cells. The supernatant was further centrifuged at 12,000 rpm for 15 min at 4°C. The supernatant (cytosolic enriched fraction) was collected. The pellet was solubilized in an equal volume of mitochondrial lysis buffer [50 mmol/L Tris (pH 7.4), 150 mmol/L NaCl, 2 mmol/L EDTA, 2 mmol/L EGTA, 0.2% Triton X-100, and 0.3% NP40] supplemented with 1× protease inhibitor cocktail and 250 μmol/L phenylmethylsulfonyl fluoride. Mitochondrial extracts were recovered by centrifugation at 12,000 rpm for 15 min at 4°C. Cytosolic and mitochondrial fractions (50 μg) were subjected to SDS-PAGE and immunoblotting.

Western Blotting

Cells were harvested in 200 μL radioimmunoprecipitaton assay buffer [150 mmol/L NaCl, 1% Triton X-100, 0.1% SDS, 10 mmol/L Tris (pH 7.5), 1% deoxycholate] with 1× protease inhibitor cocktail (Roche Diagnostics) and 1 mmol/L phenylmethylsulfonyl fluoride, and lysates were stored at -20°C. After sonication and protein determination using the Pierce BCA kit (Pierce), equal amounts of protein (50 μg) were subjected to 12% to 15% SDS-PAGE and electroblotted onto Immuno-P Transfer Membrane (Millipore). After blocking nonspecific binding sites with 5% fat-free milk in PBS with 0.1% Tween 20 for 1 h, the membranes were incubated with the indicated primary antibody overnight at 4°C. After washes in PBS with 0.1% Tween 20, membranes were incubated with the corresponding horseradish peroxidase–conjugated anti-rabbit or anti-mouse secondary antibody. Signal was detected by chemiluminescence using SuperSignal reagent (Pierce).

Flow Cytometric Analysis

Cells (1×10^6 per assay) were resuspended in 100 μL of 1× Annexin V labeling buffer [10 mm/L HEPES/NaOH (pH 7.4), 140 mm/L NaCl, 5 mm/L $CaCl_2$] with 2 μL Annexin V-Fluos (Roche Diagnostics), and 2 μL propidium iodide (Sigma-Aldrich, 50 μg/mL) and incubated for 15 min at room temperature. The percentage of apoptotic cells with Annexin V–positive/propidium iodide–negative was measured using FACScan flow cytometer (Becton Dickinson) and CellQuest software(Becton Dickinson). For measurement of mitochondrial transmembrane potential ($\Delta\Psi_m$; ref. 32), cells were resuspended in 1 mL serum-free medium containing cationic fluorescent dye tetramethylrhodamine ethyl ester (final concentration, 25 nmol/L; Molecular Probes), which normally accumulates in mitochondria as a direct function of $\Delta\Psi_m$, and incubated at 37°C for 20 min in the dark. After washing twice with PBS, fluorescence in cells was immediately measured in a flow cytometer.

Lentiviral Vector Construction for RNA Interference

Two lentiviral vectors, pLL3.7-sh-casp-2 and pLL3.7-sh-casp-9, were generated to produce short hairpin RNA (shRNA) directed against human caspase-2 or caspase-9 mRNA, respectively, for expression of small interfering RNA (siRNA). Briefly, they were derived from the pLL3.7 plasmid (a gift from Luk Van Parijs, Department of Biology, Massachusetts Institute of Technology), which carries a cytomegalovirus promoter driving expression of enhanced green fluorescent protein and the mouse U6 promoter for downstream shRNA synthesis (33). A sequence, ACAGCTGTTGTTGAGCGAA (19) or CCAGGCAGCTGATCATAGA (34), known to silence human caspase-2 or caspase-9 as a siRNA, was adapted with a loop sequence (35) and then inserted into pLL3.7 vector, respectively, to create a shRNA.

Viral Production and Cell Infections

Lentiviral production was done following the guidelines of the ViraPower Lentiviral Expression System (Invitrogen). Briefly, we using LipofectAMINE 2000 (Invitrogen) cotransfected plasmid pLL3.7 and packaging vectors into 293FT cells and collected the resulting supernatant after 36 h. We recovered virus after ultracentrifugation for 1.5 h at 25,000 rpm in a Beckman SW28 rotor and resuspension in PBS (15-200 μL). Titers were determined by infecting 293FT cells with serial dilutions of concentrated lentivirus. We determined enhanced green fluorescent protein expression of infected cells by flow cytometry 48 h after infection. We usually obtained titers ranging from 4×10^8 to 10×10^8 viral units/mL. To high efficiently infect multiple myeloma cells, 1×10^6 cells were cultured in 1 mL Opti-MEM I reduced serum medium (Invitrogen) supplemented with 10×10^6 to 50×10^6 lentiviral particles (multiplicity of infection, 10-50) and 10 μg/mL polybrene (Sigma-Aldrich) and spun at 1,200 rpm for 1 h at 30°C in a Beckman Allegra 6R centrifuge. Supernatant was removed after infection and replaced with growth medium for experiments after 72 h.

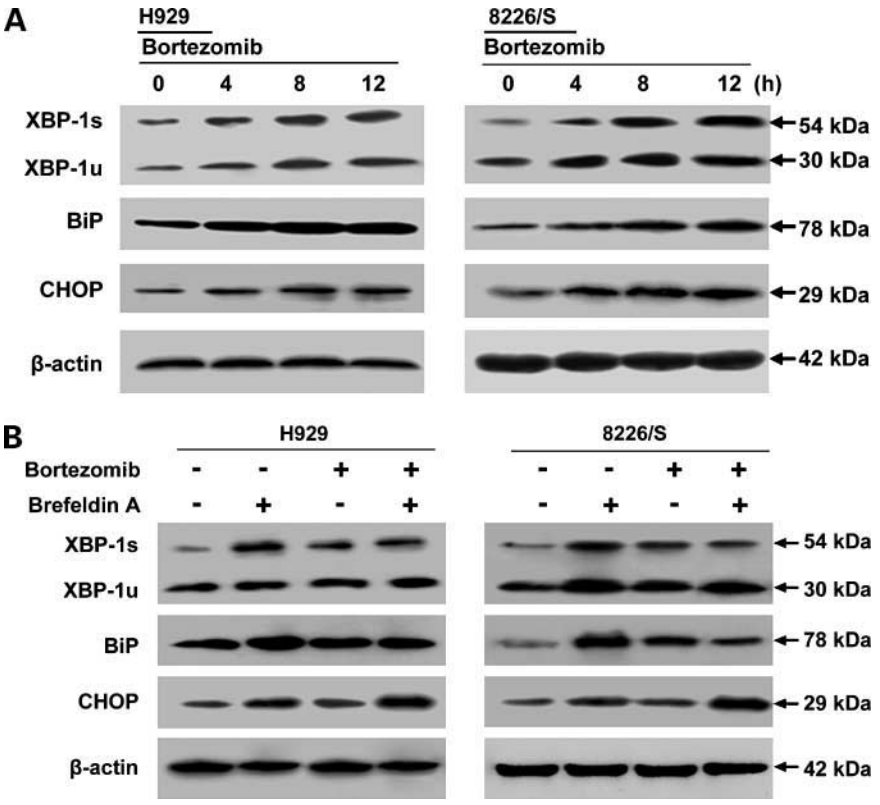

Figure 1. Bortezomib evokes ER stress but disrupts brefeldin A–induced UPR in myeloma cells. **A,** cells were exposed to bortezomib (100 and 50 nmol/L for H929 and 8226/S cells, respectively) or brefeldin A (600 and 300 ng/mL for H929 and 8226/S cells, respectively) for the indicated times. **B,** H929 and 8226/S cells were incubated with bortezomib (100 and 50 nmol/L, respectively) for 12 h in the presence or absence of brefeldin A (600 and 300 ng/mL, respectively). The cells were preincubated with bortezomib for 2 h and then further treated with brefeldin A for 10 h. The expression levels of key regulators of the ER stress response or UPR were analyzed. Protein expression was determined in cell lysates subjected to SDS-PAGE and immunoblotting with the indicated antibodies. β-Actin was used as a control for protein loading.

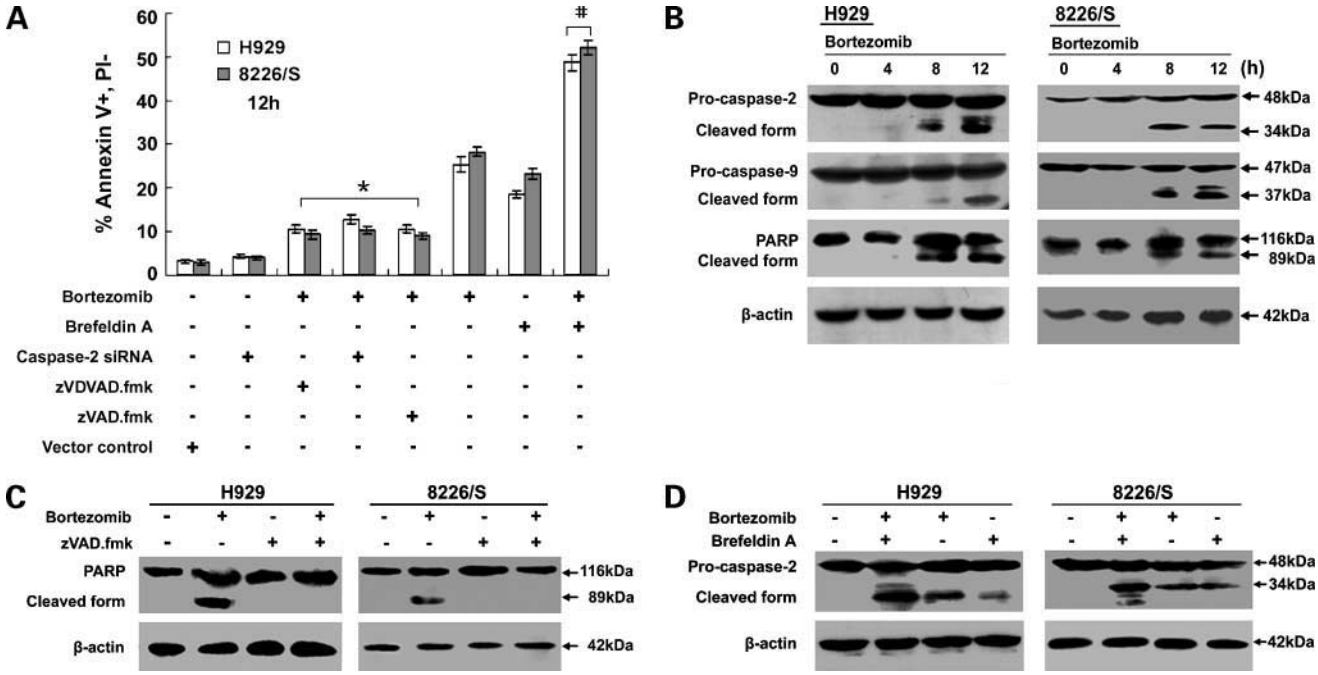

Figure 2. Bortezomib-induced caspase-2 activation and apoptosis in myeloma cells involves ER stress response. **A,** cells were treated with bortezomib (100 and 50 nmol/L for H929 and 8226/S cells, respectively) for 12 h in the presence or absence of brefeldin A (600 and 300 ng/mL for H929 and 8226/S cells, respectively) or 2 h preincubation of caspase inhibitors (10 μmol/L zVAD.fmk or 10 μmol/L zVDVAD.fmk or 10 μmol/L zLEHD.fmk) or knockdown of caspase-2 (expression of caspase-2 siRNA). The percentage of apoptotic cells (Annexin V–positive/propidium iodide–negative) was analyzed by flow cytometry. *Columns,* mean of at least three independent experiments; *bars,* SD. *, $P < 0.05$, compared with bortezomib alone; #, $P < 0.05$, compared with bortezomib or brefeldin A alone. **B,** H929 and 8226/S cells were treated with 100 and 50 nmol/L bortezomib, respectively, for indicated times. **C,** cells were treated with bortezomib (100 and 50 nmol/L for H929 and 8226/S cells, respectively) for 12 h with or without preincubation of pan-caspase inhibitor (10 μmol/L zVAD.fmk) for 2h. **D,** cells were incubated with bortezomib (100 and 50 nmol/L for H929 and 8226/S cells, respectively) for 12 h with or without brefeldin A (600 and 300 ng/mL for H929 and 8226/S cells, respectively). The poly(ADP-ribose) polymerase cleavage and processing of caspase-2 and caspase-9 were determined, respectively, in cell lysates subjected to SDS-PAGE and immunoblotting with the indicated antibodies. β-Actin was used as a control for protein loading.

Statistical Analysis

All experiments, except immunoblots, were done in triplicate, and the results were expressed as mean ± SD and analyzed by the Student's *t* test. Statistical significance was defined as $P < 0.05$.

Results and Discussion

Bortezomib Induces ER Stress-Initiated Apoptosis

H929 and 8226/S cells were exposed to various concentrations of bortezomib. The growth inhibition curves were shown for the two cell lines (Supplementary Fig. S1A and B).[1] The IC_{50} values of bortezomib were 118 and 55 nmol/L for H929 and 8226/S cells, respectively. The IC_{50} concentrations of brefeldin A were 606 ng/mL in H929 cells and 284 ng/mL in 8226/S cells. To compare the proapoptotic effect of bortezomib and brefeldin A, the cells were treated with the approximate IC_{50} concentration of bortezomib (100 or 50 nmol/L) and brefeldin A (600 or 300 ng/mL) for H929 and 8226/S cells, respectively. The percentage of apoptotic cells with Annexin V–positive/propidium iodide–negative was evaluated at indicated times by flow cytometer. Bortezomib was more effective in inducing apoptotic cell death than brefeldin A (Supplementary Fig. S1C and D).[1] Because the approximate C_{50} values of bortezomib and brefeldin A can effectively trigger apoptosis in H929 and 8226/S cells, respectively, subsequent experiments were carried out using these concentrations of each drug.

Multiple myeloma cells produce large amounts of protein, namely immunoglobulin, the maturation and folding of which relies on the activity of ER-resident chaperones and folding enzymes. ER proteins (immunoglobulin subunits) that fail to fold properly are degraded by the 26S proteasome or ER-associated protein degradation system. Suppression of proteasome activity induces the accumulation of ER-associated protein degradation substrates (unfolded immunoglobulin subunits) in the ER, thereby inducing severe ER stress and UPR coupled with the induction of apoptosis (12, 16, 17). The induction of BiP (a chaperone resided in ER), CHOP (a basic-region leucine zipper transcriptional factor associated with ER stress-induced apoptosis), and XBP-1 (a basic-region leucine zipper transcriptional factor) is an established marker for the presence of ER stress response or UPR (17, 36, 37). Of

[1] Supplementary materials for this article are available at Molecular Cancer Therapeutics Online (http://mct.aacrjournals.org/).

note, prosurvival UPR components including BiP and XBP-1s (active spliced form of XBP-1) is necessary to protect plasma cells from stress-induced apoptosis, whereas proapoptotic UPR component CHOP leads to induction of apoptosis. A recent study reported that 26S proteasome inhibitor bortezomib triggered severe ER stress response or UPR associated with apoptosis in multiple myeloma cell lines (17). To further investigate this possibility, we examined the effects of bortezomib on the expression of proteins that are modulated by classic inducer of ER stress in other model system (24). In these experiments, the ER-Golgi transport inhibitor brefeldin A served as positive controls for ER stress response or UPR. Consequently, immunoblotting analysis showed that bortezomib, like classic ER stress inducer brefeldin A (Supplementary Fig. S2),[1] induced a time-dependent expression of representative UPR target genes such as BiP and CHOP (Fig. 1A) and simultaneously activated the important UPR regulator XBP-1 (Fig. 1A), as evidenced by the conversion of a 267–amino acid unspliced XBP-1 (XBP-1u) to a 371–amino acid spliced XBP-1 (XBP-1s) as reported previously (36, 37), all of which are indicative of ER stress. Our results therefore confirmed bortezomib-induced ER stress response or UPR in H929 and 8226/S cells. Surprisingly, however, bortezomib treatment blocked rather than further augmented the induction of brefeldin A–induced BiP and XBP-1s (Fig. 1B), resulting in enhanced apoptosis (Fig. 2A), raising the possibility that bortezomib might evoke severe ER stress but cripple the prosurvival UPR required. Our results are consistent with the studies showing that proteasome inhibitors disrupt the UPR (37). Thus, the mechanisms by which bortezomib induces apoptosis of multiple myeloma cells appear to be associated with the expression imbalance between proapoptotic and prosurvival UPR components.

Caspase-2 Activation Is Required for ER Stress-Induced Apoptosis by Bortezomib

To further determine whether ER stress-induced apoptosis by bortezomib in multiple myeloma cells involves caspase cascade, we simultaneously analyzed the cleavage of the caspase substrate poly(ADP-ribose) polymerase and the effect of the broad-spectrum caspase inhibitor zVAD.fmk on apoptotic cell death in H929 and 8226/S cells. As shown here, treatment with bortezomib alone resulted in a time-dependent cleavage of full-length poly(ADP-ribose) polymerase (Fig. 2B) and increase in the percentage of apoptotic cells with Annexin V–positive/propidium iodide–negative (Fig. 2A), which were blocked by means of peptide-mediated inactivation of caspases (Fig. 2A and C). These data confirmed that caspases were activated in H929 and 8226/S cells during bortezomib-induced apoptotic programs, thereby prompting us to further investigate whether caspase-2 activation is also involved in bortezomib-induced apoptosis in multiple myeloma cells because initiator caspase-2 is a central component of most model of ER stress-induced apoptosis (22–26), and bortezomib-triggered apoptosis is closely associated with ER stress, as confirmed by our and other findings (Fig. 1A; Supplementary Fig. S2; [1] ref. 17). The processing of pro-caspase-2 was analyzed in total extracts from H929 and 8226/S cells exposed to bortezomib in the presence or absence of the ER stress inducer brefeldin A. As expected, treatment with bortezomib alone resulted in pro-caspase-2 processing and apoptosis induction in a time-dependent manner (Fig. 2B; Supplementary Fig. S1C).[1] Moreover, brefeldin A alone also led to the activation of caspase-2 (Fig. 2D). Most importantly, bortezomib acted synergistically with brefeldin A to induce apoptotic cell death (Fig. 2A) and the activation

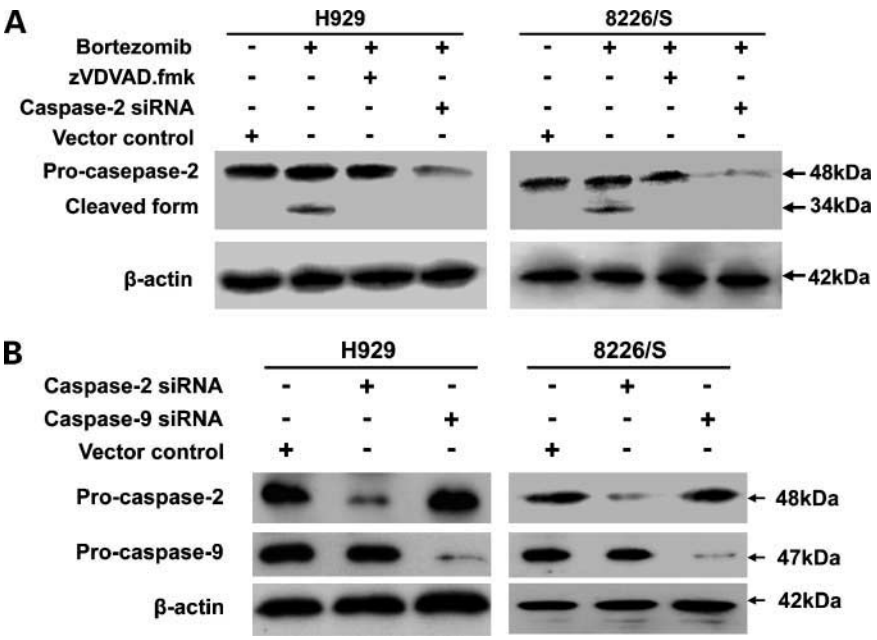

Figure 3. Bortezomib induces caspase-2-dependent apoptosis in myeloma cells. **A,** H929 and 8226/S cells were treated with 100 and 50 nmol/L bortezomib, respectively, for 12 h in the presence or absence of pretreatment of caspase-2 inhibitor (10 μmol/L zVDVAD.fmk) or caspase-2 knockdown. **B,** H929 and 8226/S cells were infected with lentivirus producing enhanced green fluorescent protein and shRNA for expression of siRNA to knockdown of caspase-2 or caspase-9. The caspase-2 or caspase-9 siRNA-expressing cells was collected by sorting of enhanced green fluorescent protein–positive cells. The processing and expression levels of caspases were determined, respectively, in cell lysates subjected to SDS-PAGE and immunoblotting with the indicated antibodies. β-Actin was used as a control for protein loading.

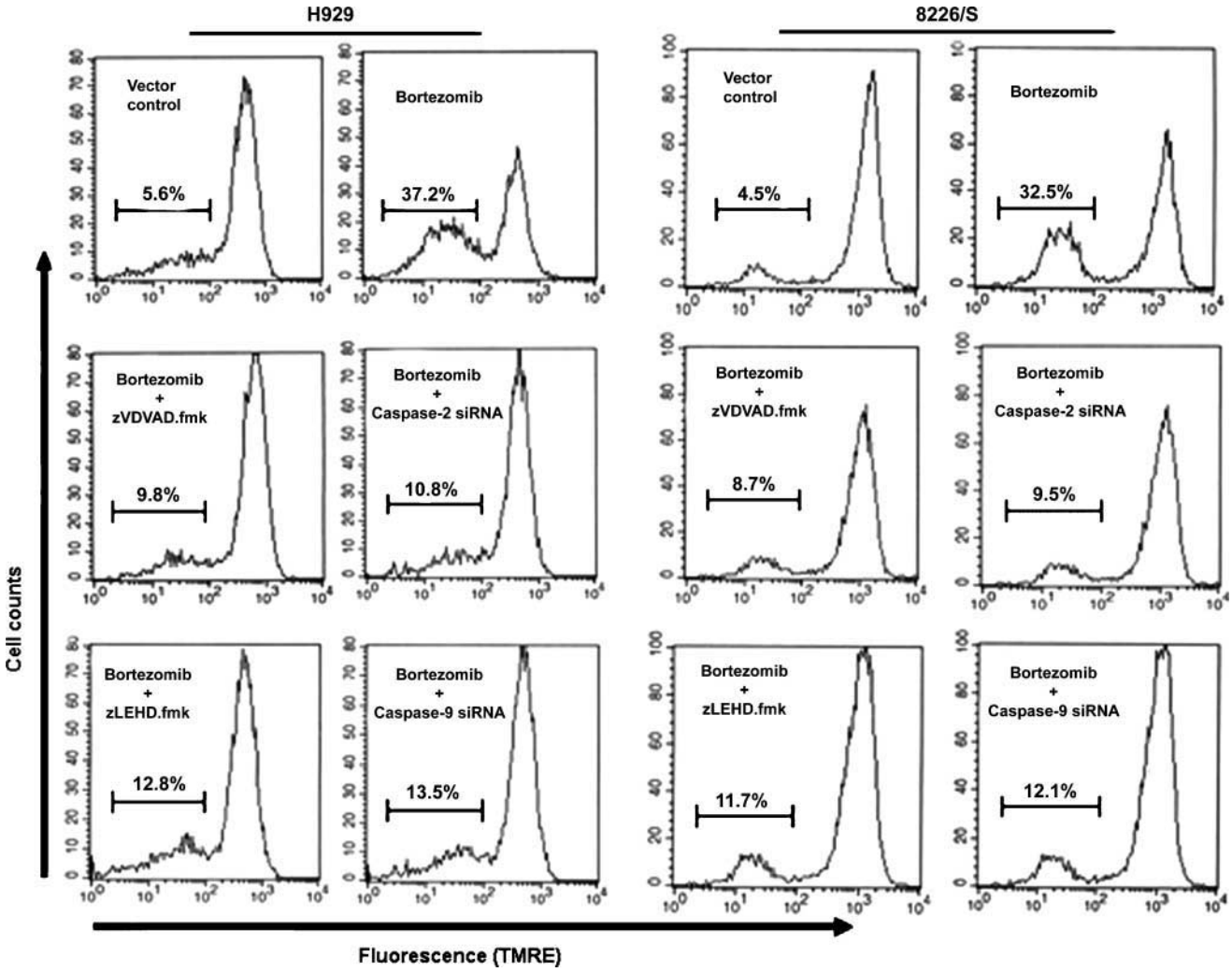

Figure 4. Requirement of caspase-2 and caspase-9 for bortezomib-induced loss of $\Delta\Psi_m$ in myeloma cells. The cells were treated with bortezomib (100 and 50 nmol/L for H929 and 8226/S cells, respectively) for 12 h in the presence or absence of 2 h preincubation of caspase inhibitors (10 μmol/L zVDVAD.fmk or 10 μmol/L zLEHD.fmk) or knockdown of caspase-2 or caspase-9 (expression of caspase-2 or caspase-9 siRNA). $\Delta\Psi_m$ was measured by tetramethylrhodamine ethyl ester (*TMRE*) fluorescence and FACScan analysis. The histogram and percentages of $\Delta\Psi_m$ reduction are shown.

of caspase-2 (Fig. 2D) as evidenced by cleavage of the precursor species. To determine whether our results can be generalized, we did experiments wherein both H929 and 8226/S cells were treated with bortezomib in the presence or absence of another ER stress inducer tunicamycin. As shown in Supplementary Fig. S3,[1] this treatment resulted in a synergistic effects on apoptosis induction and caspase-2 processing comparable with treatment with combining bortezomib and brefeldin A. Therefore, these data strongly indicated that the mechanisms underlying bortezomib-induced caspase-2 activation and apoptosis in multiple myeloma cells involve in ER stress response or UPR. To further determine the role of caspase-2 activation in bortezomib-triggered apoptotic signaling in H929 and 8226/S cells, we used a specific inhibitor of caspase-2 (zVDVAD.fmk). zVDVAD.fmk was found to block bortezomib-triggered processing of caspase-2 (Fig. 3A) and to attenuate bortezomib-induced apoptosis (Fig. 2A). To evidence these results, an lentivirus-mediated RNA interference approach was employed as detailed above. We infected H929 and 8226/S cells with lentivirus producing the shRNA specific for caspase-2 for interference with caspase-2 expression. As shown in Fig. 3B, inhibition of caspase-2 expression but not of caspase-9 expression was observed in the caspase-2 siRNA-expressing cells, which were collected by sorting of enhanced green fluorescent protein–positive cells. Consequently, impaired activation of caspase-2 and decreased induction of apoptosis were observed when compared with bortezomib alone (Figs. 2A and 3A). All together, these data strongly suggest that bortezomib-triggered apoptosis in multiple myeloma cells is dependent on the

caspase-2 activation, which closely associated with ER stress response or UPR.

Caspase-2 Activation Is Required before Mitochondrial Damage and Its Downstream Caspase-9 Activation in Bortezomib-Induced Apoptosis

To further investigate whether bortezomib-triggered apoptosis engages mitochondria-mediated apoptotic signaling, we next examined the effect of bortezomib-induced caspase-2 activation on mitochondrial permeabilization and its downstream caspase-9 activation in H929 and 8226/S cells. The irreversible caspase-2 and caspase-9 inhibitors zVDVAD.fmk and zLEHD.fmk, respectively, were used. Using the lipophilic cationic fluorochrome dye tetramethylrhodamine ethyl ester staining followed by flow cytometric analysis (32), we found that bortezomib-induced $\Delta\Psi_m$ reduction (mitochondrial depolarization) was blocked both by zVDVAD.fmk and by zLEHD.fmk (Fig. 4), whereas cytochrome *c* release was blocked by zVDVAD.fmk but not by zLEHD.fmk (Fig. 5A and B). To further confirm these results, a RNA interference approach was also used as above (Fig. 3B). Similar to inhibitor results, in H929 and 8226/S cells expressing caspase-2 or caspase-9 siRNA, bortezomib-induced $\Delta\Psi_m$ reduction was attenuated, respectively, compared with bortezomib alone (Fig. 4). Caspase-2 but not caspase-9 siRNA-expressing cells were defective in cytochrome *c* release compared with bortezomib treatment only (Fig. 5A and B). All together, our results support the studies showing that $\Delta\Psi_m$ functionally separated from cytochrome *c* release (29), and effector caspases mediates the loss of $\Delta\Psi_m$ (38). All together, these results strongly suggest that bortezomib induces a caspase-2-dependent mitochondrial apoptosis, and caspase-2 activation moreover acts upstream of mitochondria, similar to the results showing that caspase-2 is required in heat shock–induced or genotoxic stress-induced apoptosis before mitochondrial permeabilization (19–21).

To further examine the regulatory relationship between initiator caspase-2 and caspase-9 in ER stress-induced mitochondria-mediated apoptosis by bortezomib in H929 and 8226/S cells, we confirmed a time-dependent activation of caspase-2 and caspase-9 (Fig. 2B) and verified the association of caspase-2 deficiency with defective caspase-9 activation by caspase inhibitors and a RNA interference approach. We first inactivated caspase-2 and caspase-9 in multiple myeloma cells by pretreatment with zVDVAD.fmk and zLEHD.fmk, respectively. Results showed that pretreatment with zVDVAD.fmk but not with zLEHD.fmk suppressed caspase-2 processing in response to bortezomib stimulation (Fig. 6A and B). By contrast, caspase-9 activation was blocked by both zLEHD.fmk and zVDVAD.fmk (Fig. 6A and B). Therefore, caspase-2 is required for bortezomib-induced caspase-9 activation, consistent with previous studies showing that sequential caspase-2 and caspase-9 activation were shown to occur in ER stressors brefeldin A–induced and tunicamycin-induced apoptosis in HeLa cells (24). Nevertheless, we, to further confirm these results, employed a lentivirus-mediated RNA interference approach for inhibition of caspase-2 expression (Fig. 3B). As expected, impaired expression or processing of caspase-2 and caspase-9 was observed when compared

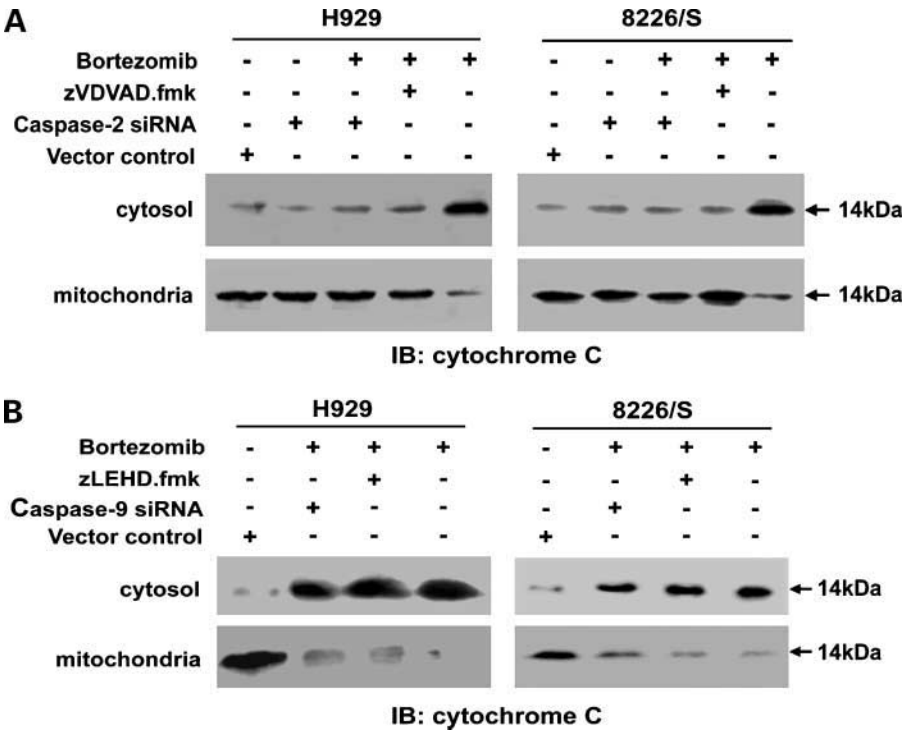

Figure 5. Cytochrome *c* release from mitochondria was determined by means of immunoblotting (*IB*) analysis of cytosolic or mitochondrial extracts (20 μg) from the cells treated with bortezomib (100 and 50 nmol/L for H929 and 8226/S cells, respectively). **A,** cells were treated with bortezomib for 12 h with or without 2 h preincubation of caspase-2 inhibitor (10 μmol/L zVDVAD.fmk) or knockdown of caspase-2. **B,** cells were treated with bortezomib with or without caspase-9 inhibitor (10 μmol/L zLEHD.fmk) or knockdown of caspase-9.

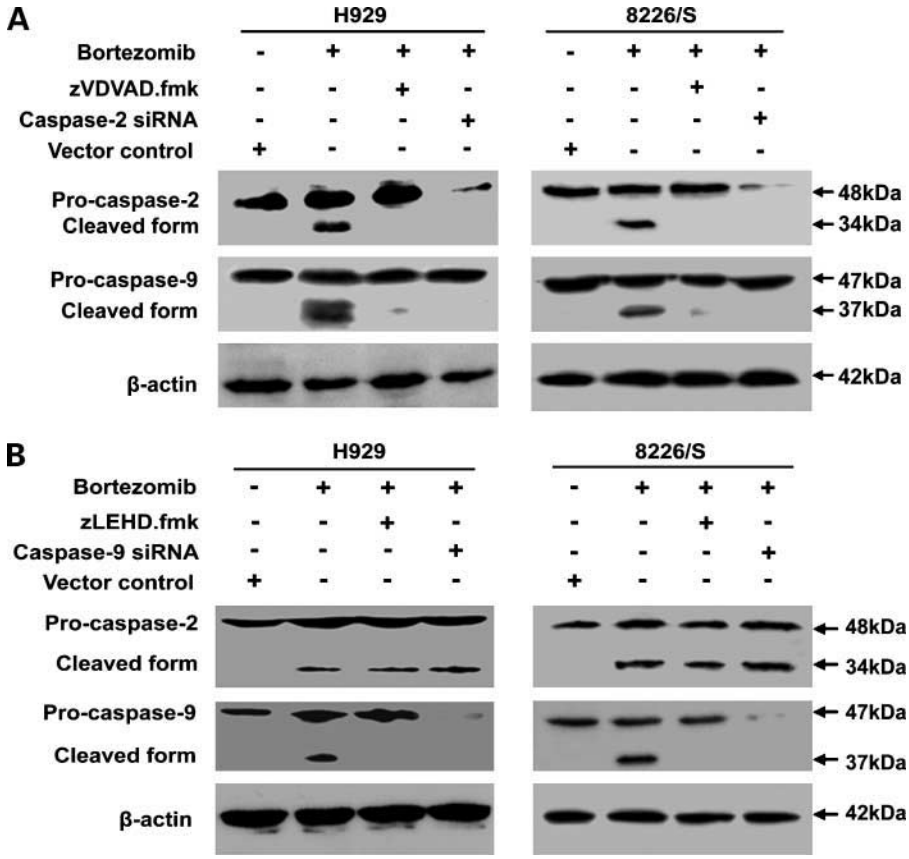

Figure 6. Regulatory relationship between caspase-2 and caspase-9 was analyzed in H929 and 8226/S cells treated with bortezomib (100 and 50 nmol/L, respectively) for 12 h (**A**) with or without 2-h preincubation of caspase-2 inhibitor (10 μmol/L zVDVAD.fmk) or knockdown of caspase-2 and (**B**) with or without 2-h preincubation of caspase-9 inhibitor (10 μmol/L zLEHD.fmk) or knockdown of caspase-9. The processing or expression levels of caspase-2 or caspase-9 was determined, respectively, in cell lysates subjected to SDS-PAGE and immunoblotting with the indicated antibodies. β-Actin was used as a control for protein loading.

with bortezomib treatment only (Fig. 6A). We also introduced the shRNA specific for caspase-9 into the cells for interference with the expression of caspase-9. Impaired activation of caspase-9 but not of caspase-2 was observed when compared with bortezomib alone (Fig. 6B). Taken together, these results therefore strongly suggest that caspase-2 as a proximal caspase acts upstream of mitochondria during ER-induced apoptosis by bortezomib in multiple myeloma cells.

Concluding Remarks

To elucidate the apoptotic mechanisms used by bortezomib, we studied the effects of this drug on ER stress-induced caspase activation and mitochondrial permeability in the initiation of cell death in human multiple myeloma cell lines. We also examined the relevance of caspase-2 to bortezomib-induced apoptotic signaling. Consequently, we showed that bortezomib treatment induced a ER stress response or UPR associated with caspase-dependent apoptosis in multiple myeloma cell lines, consistent with a previous report showing that proteasome inhibitors induce proapoptotic UPR in multiple myeloma cells (17). Surprisingly, however, bortezomib treatment blocked rather than further augmented the brefeldin A–induced stress response, leading to increased cell apoptosis. Our results are consistent with a study in multiple myeloma showing that proteasome inhibitors disrupt the UPR (37). Thus, treatment with bortezomib, which heightens ER stress in multiple myeloma cells by preventing the degradation of ER-associated protein degradation substrates, simultaneously inhibits the prosurvival UPR required, resulting in enhanced induction of caspase-dependent apoptosis. Taken together, these results point to the possibility that the mechanisms by which bortezomib induces caspase-dependent apoptosis in multiple myeloma cells is closely associated with the regulatory imbalance between proapoptotic and prosurvival UPR.

To date, the role and placement of caspase-2 within ER stress-induced apoptotic signaling remains incompletely understood. Furthermore, there is conflicting evidence of whether caspase-2 activation occurs upstream or downstream of mitochondria in stress-induced apoptosis. To further investigate relation of caspase-2 to bortezomib-triggered apoptosis in multiple myeloma cells, we using peptide- and siRNA-mediated inhibition of caspase-2 evidenced that bortezomib-triggered apoptosis is dependent on ER stress-induced caspase-2 activation and that caspase-2 is required for release of cytochrome *c*, $\Delta\Psi_m$ breakdown, and its downstream caspase-9 activation. Together, these data show that caspase-2 acts upstream of mitochondria in ER stress-initiated apoptosis by bortezomib, which is further supported by our findings that caspase-9 inhibitor or siRNA failed to block

bortezomib-induced cytochrome *c* release but did block its effect on caspase-mediated $\Delta\Psi_m$ loss. A recent report show that caspase-9 is not only required for $\Delta\Psi_m$ breakdown but also for caspase-2 activation (29), indicating that caspase-2 acts downstream of mitochondria. Although we agree with the authors in that caspase-9 regulated $\Delta\Psi_m$ loss, we argue that caspase-9 activation depends on caspase-2; moreover, caspase-2 functions upstream rather than downstream of mitochondria because caspase-2 but not caspase-9 stimulated cytochrome *c* release from mitochondria. It is possible that the discrepancies between the studies lie in differences between the model systems. Nevertheless, the present study is, to our knowledge, the first to show that caspase-2 can serve as a proximal caspase that functions upstream of mitochondrial signaling during ER stress-induced apoptosis by bortezomib in multiple myeloma cells. These novel findings, together with the fact that bortezomib inhibits the protective cellular response to genotoxic stress and potently sensitizes chemoresistant multiple myeloma cells to DNA-damaging chemotherapeutic agents (39, 40), provide mechanistic insights into apoptosis induction by proteasome inhibitors and, when extrapolated to clinic, might facilitate strategies to enhance therapeutic efficacy in multiple myeloma.

Disclosure of Potential Conflicts of Interest

No potential conflicts of interest were disclosed.

Acknowledgments

We thank Dr. Luk Van Parijs (Department of Biology, Massachusetts Institute of Technology) for providing lentiviral vector pLL3.7 and Dr. Jinyi Zhang (Samuel Lunenfeld Institute, University of Toronto) for providing lentiviral reagents and technical assistance.

References

1. Gardner RC, Assinder SJ, Christie G, et al. Characterization of peptidyl boronic acid inhibitors of mammalian 20S and 26S proteasomes and their inhibition of proteasome in cultured cells. Biochem J 2000;346:447 – 54.

2. Adams J, Palombella VJ, Sausville EA, et al. Proteasome inhibitors: a novel class of potent and effective antitumor agents. Cancer Res 1999; 59:2615 – 22.

3. Hideshima T, Richardson P, Chauhan D, et al. The proteasome inhibitor PS341 inhibits growth, induces apoptosis, and overcomes drug resistance in human multiple myeloma cells. Cancer Res 2001;61:3071 – 6.

4. Mitsiades N, Mitsiades CS, Poulaki V, et al. Molecular sequelae of proteasome inhibition in human multiple myeloma cells. Proc Natl Acad Sci U S A 2002;99:14374 – 9.

5. Chauhan D, Hideshima T, Mitsiades C, Richardson P, Anderson KC. Proteasome inhibitor therapy in multiple myeloma. Mol Cancer Ther 2005; 4:686 – 92.

6. Cavo M. Proteasome inhibitor bortezomib for the treatment of multiple myeloma. Leukemia 2006;20:1341 – 52.

7. Hideshima T, Chauhan D, Richardson P, et al. NF-κB as a therapeutic target in multiple myeloma. J Biol Chem 2002;277:16639 – 47.

8. Ma MH, Yang HH, Parker K, et al. The proteasome inhibitor PS341 markedly enhances sensitivity of multiple myeloma tumor cells to chemotherapeutic agents. Clin Cancer Res 2003;9:1136 – 44.

9. Sunwoo JB, Chen Z, Dong G, et al. Novel proteasome inhibitor PS341 inhibits activation of nuclear factor-κB, cell survival, tumor growth and angiogenesis in squamous cell carcinoma. Clin Cancer Res 2001;7: 1419 – 28.

10. Mitsiades N, Mitsiades CS, Poulaki V, et al. Biologic sequelae of nuclear factor-κB blockade in multiple myeloma: therapeutic applications. Blood 2002;99:4079 – 86.

11. Pelletier N, Casamayor-Palleja M, Luca KD, et al. The endoplasmic reticulum is a key component of the plasma cell death pathway. J Immnol 2006;176:1340 – 7.

12. Rutkowski DT, Kaufman RJ. A trip to the ER: coping with stress. Trends Cell Biol 2004;14:20 – 8.

13. Cenci S, Mezghrani A, Cascio P, et al. Progressively impaired proteasomal capacity during terminal plasma cell differentiation. EMBO J 2006;25:1104 – 13.

14. Fujita E, Kouroku Y, Isoai A, et al. Two endoplasmic reticulum-associated degradation system (ERAD) for the novel variant of the mutant dysferlin; ubiquitin/proteasome ERAD(I) and autophagy/lysosome ERAD(II). Hum Mol Genet 2007;16:618 – 29.

15. Tsai B, Ye Y, Rapoport TA. Retro-translocation of proteins from the endoplasmic reticulum into the cytosol. Nat Rev Mol Cell Biol 2002;3: 246 – 55.

16. Ferri KF, Kroemer G. Organelle-specific initiation of cell death pathways. Nat Cell Biol 2001;3:E255 – 63.

17. Obeng EA, Carlson LM, Gutman DM, Harrington WJ, Lee KP, Boise LH. Proteasome inhibitors induce a terminal unfolded protein response in multiple myeloma cells. Blood 2006;107:4907 – 16.

18. Meister S, Schubert U, Neubert K, et al. Extensive immunoglobulin production sensitizes myeloma cells for proteasome inhibition. Cancer Res 2007;67:1783 – 97.

19. Lassus P, Opitz-Araya X, Lazebnit Y. Requirement for caspase-2 in stress-induced apoptosis before mitochondrial permeabilization. Science 2002;297:1352 – 4.

20. Lin CF, Chen CL, Chang WT, et al. Sequential caspase-2 and caspase-8 activation upstream of mitochondria during ceramide and etoposide-induced apoptosis. J Biol Chem 2004;279:40755 – 61.

21. Zhivotovsky B, Orrenius S. Caspase-2 functions in response to DNA damage. Biochem Biophys Res Commun 2005;331:859 – 67.

22. Rao RV, Castro-Obregon S, Frankowski H, et al. Coupling endoplasmic reticulum stress to the cell death program. J Biol Chem 2002;277: 21836 – 42.

23. Dahmer MK. Caspase-2, -3, and -7 are involved in thapsigargin-induced apoptosis of SH-SY5Y neuroblastoma cells. J Neurosci Res 2005; 80:576 – 83.

24. Cheung HH, Kelly NL, Liston P, Korneluk RG. Involvement of caspase-2 and caspase-9 in endoplasmic reticulum stress-induced apoptosis: a role for the IAPs. Exp Cell Res 2006;312:2347 – 57.

25. Murakami Y, Alzu-Yokota E, Sonod Y, Ohta S, Kasahara T. Suppression of endoplasmic reticulum stress-induced caspase activation and cell death by the overexpression of Bcl-xL or Bcl-2. J Biochem 2007; 141:401 – 10.

26. Masud A Mohapatra A, Lakhani SA, Ferrandino A, Hakem R, Flavell RA. Endoplasmic reticulum stress-induced death of mouse embryonic fibroblasts requires the intrinsic pathway of apoptosis. J Biol Chem 2007; 282:14132 – 9.

27. Tu S, McStay GP, Boucher LM, Mak T, Beere HM, Green DR. *In situ* trapping of activated initiator caspases reveals a role for caspase-2 in heat shock-induced apoptosis. Nat Cell Biol 2006;8:72 – 7.

28. Bonzon C, Bouchier-Hayes L, Pagliari LJ, Green DR, Newmeyer DD. Caspase-2-induced apoptosis requires Bid cleavage: a physiological role for Bid in heat shock-induced death. Mol Biol Cell 2006;17: 2150 – 7.

29. Samraj AK, Sohn D, Schulze-Osthoff K, Schmitz I. Loss of caspase-9 reveals its essential role for caspase-2 activation and mitochondrial membrane depolarization. Mol Biol Cell 2006;18:84 – 93.

30. Qiang YW, Kitagawa M, Higashi M, Ishii G, Morimoto C, Harigaya K. Activation of mitogen-activated protein kinase through $\alpha_5\beta_1$ integrin is required for cell cycle progression of B progenitor cell line, Reh, on human marrow stromal cells. Exp Hematol 2000;28:1147 – 57.

31. Yeung BHY, Huang DC, Sinicrope FA. PS-341 (bortezomib) induces lysosomal cathepsin B release and a caspase-2-dependent mitochondrial permeabilization and apoptosis in human pancreatic cancer cells. J Biol Chem 2006;281:11923 – 32.

32. Schmidt-Mende J, Gogvadze V, Hellstrom-Lindberg, Zhivotovsky B. Early mitochondrial alterations in ATRA-induced cell death. Cell Death and Differ 2006;13:119 – 28.

33. Rubinson DA, Dillon CP, Kwiatkowski AV, et al. A lentivirus-based system to functionally silence genes in primary mammalian cells, stem cells and transgenic mice by RNA interference. Nat Genet 2003;33: 401 – 6.

34. Allan LA, Clarke PR. Phosphorylation of caspase-9 by CDK1/cyclin B1 protects mitotic cells against apoptosis. Mol Cell 2007;26:301 – 10.

35. Brummelkamp TR, Bernards R, Agami R. A system for stable expression of short interfering RNAs in mammalian cells. Science 2002; 296:550 – 3.

36. Carrasco DR, Sukhdeo K, Protopopova M, et al. The differentiation and stress response factor XBP-1drives multiple myeloma pathogenesis. Cancer Cell 2007;11:349 – 60.

37. Lee AH, Iwakoshi NN, Anderson KC, Glimcher LH. Proteasome inhibitors disrupt the unfolded protein response in myeloma cells. Proc Natl Acad Sci U S A 2003;100:9946 – 51.

38. Lakhani SA, Musud A, Kuoda K, et al. Caspase-3 and 7: key mediators of mitochondrial events of apoptosis. Science 2006;311: 847 – 51.

39. Mitsiades N, Mitsiades CS, Richardson PG, et al. The proteasome inhibitor PS-341 potentiates sensitivity of multiple myeloma cells to conventional chemotherapeutic agents: therapeutic applications. Blood 2003;101:2377 – 80.

40. Orlowski RZ, Nagler A, Sonneveld P, et al. Randomized phase III study of pegylated liposomal doxorubicin plus bortezomib compared with bortezomib alone in relapsed or refractory multiple myeloma: combination therapy improves time to progression. J Clin Oncol 2007;25:3892 – 901.

Molecular Cancer Therapeutics

Caspase-2 functions upstream of mitochondria in endoplasmic reticulum stress-induced apoptosis by bortezomib in human myeloma cells

Hongtao Gu, Xiequn Chen, Guangxun Gao, et al.

Mol Cancer Ther 2008;7:2298-2307.